Dueling timescales of host movement and disease recovery determine invasion of disease in structured populations

PAUL C. CROSS[1,2], JAMES O. LLOYD-SMITH[1,3], PHILIP L. F. JOHNSON[3] & WAYNE M. GETZ[1,2]

[1] Department of Environmental Science, Policy and Management, University of California at Berkeley

[2] Mammal Research Institute, Department of Zoology and Entomology, University of Pretoria, South Africa

[3] Biophysics Graduate Group, University of California at Berkeley

Addresses:

James Lloyd-Smith, 299 Life Sciences Addition, Berkeley CA 94720-3200

Philip Johnson, 299 Life Sciences Addition, Berkeley CA 94720-3200

Wayne Getz, 140 Mulford Hall #3114, Berkeley CA 94720-3112.

Author for correspondence: Paul Cross, 140 Mulford Hall #3114, Berkeley CA 94720-3112. E-mail: pcross@nature.berkeley.edu

Word Count: 4773 excluding references, figure legends, and supplementary material

Abstract

The epidemic potential of a disease is traditionally assessed using the basic reproductive number, R_0. In populations with social or spatial structure, however, a chronic disease is more likely to invade than an acute disease with the same R_0, because it persists longer within each group and allows for more host movement between groups. Acute diseases 'perceive' a more structured host population, and it is more important to consider host population structure in analyses of these diseases. The probability of a pandemic does not arise independently from characteristics of either the host or disease, but rather from the interaction of host movement and disease recovery timescales. The R_* statistic, a group-level equivalent of R_0, is a better indicator of disease invasion in structured populations than the individual-level R_0.

INTRODUCTION

At the turn of the 20th century, rinderpest swept through Africa, devastating populations of African buffalo and wildebeest (Sinclair 1977; Plowright 1982; Anderson 1995). From 1929 to 1983 recurrent rinderpest outbreaks occurred in the buffalo and eland populations of Central and Eastern Africa, while many other ungulate species, such as duikers, steenbok, oribi, roan, sable and gerenuk, were relatively unaffected (Anderson 1995). Why were some hosts affected more than others? Traditionally, this may have been explained by immunological differences in susceptibility. We illustrate, however, a significant component of behavioral susceptibility exists that is not a simple function of group size or population density, but rather the interaction of group size and host movement.

Risk of disease is assumed to be a significant cost of group living (Freeland 1976; Moller *et al.* 1993), yet recent comparative analyses that investigated the effect of group size on the immune system or parasite diversity have had mixed results (Cote & Poulin 1995; Nunn *et al.* 2000; Nunn 2002; Stanko *et al.* 2002; Tella 2002; Nunn *et al.* 2003a; Nunn *et al.* 2003b). These mixed results may be due, in part, to the interaction of movement and group size, whereby reduced movement rates can mitigate some costs associated with larger group sizes. Specifically, large groups will be exposed to fewer introductions of disease if movement between groups is sufficiently rare.

Several recent theoretical studies have investigated the role of host population structure in the invasion or persistence of disease (Hess 1996; Swinton *et al.* 1998; Keeling 1999; Keeling & Gilligan 2000; Keeling & Grenfell 2000; Thrall *et al.* 2000; Park *et al.* 2001; Fulford *et al.* 2002; Keeling & Rohani 2002; Park *et al.* 2002;

Hagenaars *et al.* 2004). These studies incorporated host movement into structured disease models either phenomenologically or mechanistically. Models with mechanistic host movement explicitly move individuals from one group to another (e.g. Hess 1996; Thrall *et al.* 2000; Keeling & Rohani 2002). Models with phenomenological host mixing assume that hosts do not move between groups but can infect others within and among groups simultaneously (e.g. Ball *et al.* 1997; Swinton *et al.* 1998; Hagenaars *et al.* 2004). The phenomenological approach may be appropriate for plant-pathogen systems (e.g. Park *et al.* 2001; Park *et al.* 2002), but can obscure the relationships between host movement, group size, and disease recovery in mobile host populations. For example, in a system where between-group movements are rare, an epidemic of an acute, highly-transmissible disease may run to completion within a group before any individual moves and spreads infection to a new group. A mechanistic model more readily captures this possibility, while a model with phenomenological mixing between groups does not. In this study, we investigate how the interactions of group size, movement and recovery affect the probability of invasion by disease into structured populations using a mechanistic mixing model.

Lloyd-Smith *et al.* (2004) showed that transmission of sexually-transmitted diseases is well-described by a phenomenological mixing model when partner exchange is very rapid relative to the infectious period, and otherwise a mechanistic pair-formation model is required. Keeling and Rohani (2002) reached similar conclusions for a two-patch system where host mixing was frequent. We expand upon these analyses by exploring a broad range of relative timescales of movement and disease recovery as well as group and population size. Our analysis is motivated by questions regarding the

invasion of disease in wildlife populations where host movement between groups can be rare or relatively frequent (e.g. natal dispersal versus frequent fission and fusion of entire groups), infectious periods range from several days to several years (e.g. rabies versus bovine tuberculosis), and group sizes range from monogamous pairs to thousands of individuals. We focus on directly-transmitted diseases where hosts may move among groups, but contacts that are sufficient for disease transmission occur only within a group. These groups may reflect either social or spatial structure in the host population.

The basic reproductive number, R_0, is the expected number of infections caused by a typical infectious individual in a completely susceptible population (Anderson & May 1991). The R_0 statistic has been the traditional standard by which epidemiologists and disease ecologists quantify the potential growth of a disease (Anderson & May 1991; Diekmann & Heesterbeek 2000). In stochastic models, a disease cannot invade the entire system when $R_0 \leq 1$ and has a non-zero probability of invading only when $R_0>1$. In the simplest case of an SIR (Susceptible-Infected-Recovered) disease (Anderson & May 1991), R_0 is the ratio of two rates, or timescales: the infection rate and the recovery rate. If transmission is density independent, with rate parameter β, and the recovery rate γ is constant, then $R_0 = \beta/\gamma$ (McCallum *et al.* 2001). Further, the average length of the infectious period is $1/\gamma$. We use a stochastic metapopulation model to illustrate the importance of another ratio of two timescales, specifically the ratio of the rates at which hosts move between groups (μ) and recover from disease (γ). For the simple case of constant recovery and no mortality, this ratio, μ/γ, is the expected number of times an infectious individual will move between groups.

First, we describe the simulation model and explore how the interactions of group size, host movement, and infectious period affect the probability of invasion by a disease. Next, we describe a relatively new metric of disease invasion, R_*, which is the number of groups that are expected to become infected from the initially infected group (Ball *et al.* 1997). In other words, R_* is the group-level analogue of R_0. We then use the simulation model to estimate R_0 and R_* and demonstrate that R_* is a better predictor of disease invasion in structured populations with mechanistic host movement between groups. We conclude with a number of testable predictions that follow from the ideas presented here.

DEMONSTRATION OF DUELING TIMESCALES EFFECT

We use an individual-based, stochastic, discrete-time SIR model to investigate how the dueling timescales of host movement and disease recovery affect the ability of a directly-transmitted disease to invade a spatially, or socially, structured population. The total host population is evenly divided into an array of groups. The host population is further subdivided into susceptible, infected, and recovered classes where S, I, and R are respectively the number of hosts in each category. Three processes are described in the model: movement between groups, infection, and recovery of infected hosts. Since the intent of the model is a qualitative description of different interactions, we have simplified these processes as much as possible. For the case presented here, we consider a successful invasion to have occurred when the disease becomes a pandemic and infections occur within all groups of a structured population. This narrow definition does not count disease establishment within a single patch as an invasion, but instead

emphasizes the spread of the disease among groups which is the phenomenon of interest here.

We assume that movement between groups is density independent, and all individuals have a constant probability, μ, of leaving their current group each time step. Groups are organized on a square lattice and individuals can only move to their four nearest-neighboring groups. To avoid boundary effects, opposite edges of the array are connected to create a torus. In the supplementary material, we expand the analysis to include a loop structure, where each group has only two nearest-neighbors, and a spatially implicit array, where individuals can move to any other group within a time step (equivalent to the 'island' model used previously (Hess 1996; Fulford *et al.* 2002)). We assume that infected individuals recover to an immune class with a constant probability, γ, per time step.

To isolate the effects of host movement and facilitate the comparison of disease dynamics in a range of population structures, we assume disease transmission is frequency-dependent (Getz & Pickering 1983). Thus the probability of infection per time step for each susceptible in group i is given by the expression $1-\exp\left(-\beta\frac{I_i}{N_i}\right)$, where β is the transmission coefficient, I_i is the number of infected individuals in group i, and N_i is the total number of individuals in group i. Since we do not incorporate host demographic dynamics, the assumption of frequency-dependent rather than density-dependent transmission represents a rescaling of the transmission coefficient β. If contact or transmission rates increase with population density (McCallum *et al.* 2001), then disease invasion would be even less likely when the population is divided into many

small groups than indicated by results presented here, but our overall conclusions about the interaction of movement and recovery timescales would still hold.

In a continuous-time model with frequency-dependent transmission and a constant recovery rate, $R_0 = \beta/\gamma$ (Anderson & May 1991; McCallum *et al.* 2001). For the discrete-time model used here, β/γ is an approximation of R_0, which works well when the probability of infection per timestep is small and group sizes are relatively large. The approximation does not change our qualitative conclusions, however, so for clarity we refer to the ratio β/γ as R_0. We also assume that disease invasion is fast relative to birth and death rates, so the total population size is constant. Each simulation starts with one infected individual, and all groups begin with the same number of individuals. Since our spatial model was symmetric, group sizes remained relatively constant during the course of each run.

We begin by comparing the dynamics of two diseases with the same R_0 value (β/γ) but where one disease is slow (i.e. a chronic disease with a relatively long infectious period; $\beta = 0.05$, $\gamma = 0.01$) while the other is an order of magnitude faster ($\beta = 0.5$, $\gamma = 0.1$). For time steps of 1 day, these parameters correspond to mean infectious periods of 100 or 10 days, respectively. We simulated the invasion of these two diseases in three different host population structures: 1 group of 1000 individuals (equivalent to the common "mean-field approximation" of random mixing among all individuals), 25 groups of 40 individuals, and 100 groups of 10 individuals.

As expected, subdividing the population into more groups decreases the probability of pandemic (Wilson & Worcester 1945) because it decreases the average group size and increases the number of between-group jumps the disease must make to

penetrate the entire population. A less obvious effect is that slower diseases are more likely to invade a structured population, even if they have the same R_0 as a faster disease. For the case of 100 groups of ten individuals, the slow disease ($\gamma = 0.01$, $\beta = 0.05$) infected, on average, far more individuals than the fast disease ($\gamma = 0.1$, $\beta = 0.5$) before the disease died-out (658 ± 45 SE compared to 19 ± 2.3 SE; Fig. 1). This typifies the interaction of the host movement and disease recovery timescales: diseases with longer infectious periods allow more time for host mixing to occur and thus experience populations that are effectively larger. When the movement rate is zero, neither a fast nor slow disease will invade the entire population regardless of the value of R_0. When movement is very frequent, both the fast and the slow disease are likely to invade the structured population provided that $R_0>1$.

The simulated epidemics in the one-group and 100-group populations differ markedly, but were less different for the slow disease compared with the fast disease. In other words, approximating a structured population by a mean-field model (i.e. a single group with homogenous mixing of hosts) is more appropriate for slow diseases than fast diseases (Fig. 1; Cross 2004). The faster the disease, the more important it is to incorporate the spatial/social structure into any analysis. The mean infectious period ($1/\gamma$) defines the natural disease timescale, and when movement occurs on this timescale or slower then movement should be incorporated mechanistically, rather than phenomenologically.

INSERT FIGURE 1

Next we examine a range of host movement and recovery probabilities. The proportion of the population infected over the course of an epidemic depends on the expected number of group changes per infectious lifetime (μ/γ), on R_0 (β/γ), and on group size (Fig. 2). When movement is infrequent relative to the recovery rate, R_0 has little predictive ability because few infections result for all values of R_0 (Fig. 2a). If movement is frequent relative to recovery, increasing R_0 increases the average proportion of the population that becomes infected (Fig. 2a), consistent with predictions from mean-field models (Anderson & May 1991; Diekmann & Heesterbeek 2000). Increasing the host group size decreases the amount of host movement required for the disease to invade the entire population (Fig. 2b). Larger groups experience larger within-group outbreaks, and hence more infected individuals dispersing from each infected group (given density-independent movement). For our model with frequency-dependent transmission, the total number of infected individuals is, on average, a fixed proportion of group size; for density-dependent transmission, the proportion infected would increase with group size, causing greater increases in the number of infected dispersers.

For high values of R_0, the ratio μ/γ yields a sharp threshold for invasion (Fig. 2b). As a rule of thumb, a disease will invade the metapopulation if μ/γ is greater than the reciprocal of the expected number of individuals that will be infected within a single group. This makes intuitive sense because in this model system μ/γ is the expected number of between-group movements made by each infectious individual. Thus, μ/γ multiplied by the expected number of infected individuals is the expected number of infected dispersers per group—which must exceed one for a pandemic. When R_0 is high, almost all individuals in a group will be infected, so for a pandemic μ/γ should be greater

than the reciprocal of the average group size. For example, if the group size is 200, then, on average, more than one infectious individual in 200 will need to move between groups (i.e. $\mu/\gamma > 0.005$) for a pandemic to occur.

INSERT FIGURE 2

The mean proportion of the population that becomes infected, shown in Fig. 2, obscures the underlying distribution of the number of infections per epidemic (i.e. over different runs of the stochastic simulation). It is incorrect to assume that the mean of this distribution is similar to the median or mode, because in many cases the distribution is bimodal with peaks centered on zero and one or close to one (Fig. 3c, f, i). When movement is very infrequent relative to recovery, the probability of a pandemic is close to zero because the disease almost always dies out within the initial group (Fig. 3a,d,g). When movement is frequent, then the disease tends to either die out stochastically within the initial group or invade most or all of the metapopulation (Fig. 3 c, f, i), with the relative frequencies of die-out versus invasion determined by R_0 as in mean-field models (Diekmann & Heesterbeek 2000). With intermediate movement rates variation is considerable with regard to the extent to which the disease penetrates the population (Fig. 3b).

INSERT FIGURE 3

These results (Fig. 2a, Fig. 3) agree with previous studies when μ/γ is either much greater than one or close to zero. When μ/γ is large, then group structure of the population is less important and β/γ is a good predictor of disease invasion (Fig. 2a). When μ/γ is close to zero then β/γ is a good predictor of disease invasion within the initial group, but the probability of the spread of disease between groups is rather small. For the intermediate scenarios we analyzed, however, the ratio of movement to recovery rate (μ/γ) has greater influence on the invasion of a disease than β/γ.

PREDICTORS OF A PANDEMIC

Recent theoretical work has extended the R_0 concept to account for depletion of the susceptible pool (Keeling & Grenfell 2000), host spatial structure (Keeling 1999; Fulford *et al.* 2002), and populations with heterogeneous infectiousness or susceptibility (Diekmann & Heesterbeek 2000). However, even after incorporating these effects R_0 may be misleading in metapopulations with limited mixing, since R_0 as it is traditionally used, is an individual-based measure. Ball and colleagues demonstrated that the individual-based R_0 is not the best predictor of disease invasion in structured host populations and introduced a group-level reproductive number, R_*, which is the average number of groups infected by the initially infected group (Ball *et al.* 1997; Ball 1999; Ball & Lyne 2001; Ball & Neal 2002; Ball *et al.* 2004). This finding has been echoed in the context of reproductive fitness of a new mutant in a metapopulation (Gyllenberg & Metz 2001; Metz & Gyllenberg 2001). In a model with phenomenological mixing, $R_* > 1$ is the formal threshold criterion for invasion of a disease into an infinite number of finite-sized groups (Ball *et al.* 1997).

The phenomenological mixing model used by Ball *et al*. facilitates analysis, but to demonstrate the utility of the R_* metric in the context of interacting timescales of host movement and recovery, we applied our simulation model with explicit host movement between groups. For the model described above, we estimated R_0 and R_* by tracking the mean number of infections caused by the initially infected individual or group, respectively. Then we averaged these estimates of R_0 and R_* over many runs of the stochastic model. When a susceptible individual was infected and two or more infected individuals were present within the group, we randomly allocated the infection to only one of those infectious individuals. To estimate R_*, we tracked the number of groups that were infected by individuals that were themselves infected within the index group. Infected individuals had to move to a completely susceptible group and cause infection there in order to contribute to R_*. When individuals from multiple groups moved to a susceptible group and caused an infection, we randomly allocated the infection to one of the individuals (and thus its source group). The mean estimates over many simulations, denoted as $\hat{R}_0$ and $\hat{R}_*$, are "empirical" in the sense that they are based on data collected from simulated epidemics mimicking epidemiological contact-tracing data. As estimates from model output, they incorporate the effects of spatial structure, host movement, and depletion of the susceptible pool. Thus they will differ from traditional analytical R_0 and R_* values, which assume an infinite susceptible population and, hence, overestimate the value of these parameters when populations have a finite size.

We simulated the model using a range of transmission (β) and movement (μ) probabilities, a fixed recovery probability $\gamma = 0.1$, and an 11x11 toroidal array with ten individuals per group and nearest neighbor movement. Each parameter set was simulated

1000 times to generate mean values of $\hat{R}_0$ and $\hat{R}_*$. We then plotted the relationship between the model output variables $\hat{R}_0$, $\hat{R}_*$, and the proportion of the population infected (Fig. 4, Fig. S2.). Each line in Figure 4 corresponds to a fixed within-group transmission rate (β) and a range of movement probabilities increasing from left to right.

The empirical individual-level $\hat{R}_0$ is not a good predictor of the mean proportion infected: even when $\hat{R}_0$ is much greater than one, the mean proportion infected may be low depending upon the movement probability (Fig. 4a, Fig. S2). Also for different β, the proportion infected appears to show a threshold at different values of $\hat{R}_0$. The group-level $\hat{R}_*$, on the other hand, is a much better predictor of a pandemic in a structured population (Fig. 4b). In an idealized metapopulation, $R_* > 1$ is the threshold above which there is a finite probability of disease invasion (Ball *et al.* 1997). In our simulations, the proportion infected begins climbing at $\hat{R}_* \approx 1$ and rises most steeply around $\hat{R}_* \approx 2$ (Fig. 4b). This gradual transition around the threshold is typical of stochastic epidemic models, particularly with spatially-constrained mixing, because the invasion has many chances to die out before invading the entire population. When transmission rates (and hence R_0) are low, $\hat{R}_*$ is small for all values of movement (Fig. 4b, $\beta = 0.1$). When transmission is intermediate and movement is frequent, the disease will either stochastically die out in the initial group or invade the entire population (Fig.3d, e, f), resulting in intermediate values of $\hat{R}_*$ and mean proportion infected (Fig. 4b, $\beta = 0.5$ and 1). Finally, when both movement and transmission rates are high, $\hat{R}_*$ and the mean proportion infected are also high.

INSERT FIGURE 4

FUTURE EMPIRICAL RESEARCH

These findings suggest important directions for empirical studies, as well as a number of testable predictions. Previous analyses of disease presence/absence in different host social structures have not considered the interaction between movement rates and the duration of the infectious period (e.g. Cote & Poulin 1995; Nunn *et al.* 2000; Altizer *et al.* 2003; Nunn *et al.* 2003a; Nunn *et al.* 2003b). Our results illustrate, however, that it is the relative timescales of movement, recovery, and infection that determine the probability of a pandemic. A slow, chronic disease may "perceive" a host to be relatively well-mixed with frequent movement of individuals among groups. An acute disease will perceive that same host population to be more structured because movements between groups are less frequent relative to the timescale of the infectious period (Cross *et al.* 2004). We hypothesize that all else being equal, chronic diseases will be more likely to penetrate structured populations than acute diseases. Conversely, we hypothesize that behaviorally susceptible host species, with large groups and frequent movement, are likely to be more heavily impacted by acute diseases than hosts with small groups and infrequent movement. Thus the ratio of acute to chronic diseases found in different host populations should increase as a function of group size and movement rate.

A major focus of recent disease ecology has been how transmission or contact rates depend on population density (e.g. Bouma *et al.* 1995; Begon *et al.* 2003), but for metapopulations, we have shown that movement rates are also critical to understanding disease invasion (Figs. 2-4). Despite the importance of host movement, very few studies

have been published that examine the amount of mixing between groups of many wildlife species. Our results can help to guide the design of field studies intended to estimate host movement for disease models. The proportion of individuals that should be tracked and the duration of the study will depend upon the infectious period of the disease as well as the average group size of the host. As group sizes and infectious periods increase, the amount of movement required for a pandemic to occur decreases. Low movement rates, however, will require researchers to track more individuals to accurately estimate the amount of movement among groups. If group sizes are large, say 200, and the disease is highly infectious, say $R_0 > 5$, then only 1 in approximately 200 infectious individuals needs to switch between groups for a pandemic to become likely (Fig. 2b).

Researchers may estimate movement between groups using genetic data or tracking of known individuals (Waser *et al.* 1994; Koenig *et al.* 1996; Cain *et al.* 2003; Nathan *et al.* 2003). Radio-tracking or re-sighting data are more effective than genetic methods as long as individuals frequently move between groups relative to the duration of the study. Genetic methods of estimating movement will be relevant only for chronic diseases in large groups, and their use in a disease context involves at least three major assumptions: 1) past movement accurately reflects current movement; 2) short-term movements that are likely to be missed in genetic signatures (e.g. foraging rather than mating) are unimportant to disease dynamics; and 3) moving individuals are as reproductively successful as non-moving individuals (Waser *et al.* 1994).

FUTURE THEORETICAL RESEARCH

Our findings emphasize that the group-level reproductive number R_* is a critical determinant of invasion success in structured populations. Analytical formulations of R_* in systems with explicit host movement may clarify the important interaction between timescales of host movement and disease recovery, and help to formalize the rule of thumb proposed above. Previous work on R_* has focused on models with phenomenological host mixing and an infinite number of groups such that all new infections are in susceptible groups (Ball *et al.* 1997; Ball & Neal 2002; Ball *et al.* 2004). Analogous to recent developments in the theory of R_0 (Keeling 1999, Keeling & Grenfell 2000), further work on R_* should consider finite populations with spatial constraints on movement. Longer dispersal distances and spatial configurations that increase the number of neighboring groups (Supplementary Material) will mitigate the depletion of susceptible groups and facilitate the invasion of a disease. These effects are implicitly incorporated into our $\hat{R}_0$ and $\hat{R}_*$ estimates, but analytical exposition would help advance our understanding.

In our stochastic model, we made a number of simplifying assumptions that could be relaxed to make our simulations more realistic. First, the assumption of a constant probability of recovery per time step, γ, results in a geometrically distributed infectious period. The effects of alternative infectious period distributions on R_* are unclear (cf. Keeling & Grenfell 2000). For instance, with a fixed infectious period, time spent in the home group while infectious will increase the number of local infections, but will also diminish the infectious period in any new group, thereby decreasing the number of infections elsewhere. A fixed infectious period would also cause fewer individuals to recover before moving, compared to the geometric infectious period (with its mode at one

timestep). Second, we have assumed that movement between groups occurs instantaneously and without mortality, but if individuals spend time or die during movement their infectious lifetime within the next group is reduced, thereby decreasing R_*. Finally, we assumed that disease invasion was fast relative to the timescale of host birth and death. This is less likely to hold for chronic diseases, or for acute diseases that lead to rapid mortality rather than recovery. Both natural and disease-induced mortality shorten the infectious period and thus reduce R_0 (Anderson & May 1991) and R_*. Our broad conclusions about the interaction of host movement and disease recovery timescales should still apply, but investigating the effects of host demographics and disease mortality on R_* would be an important extension of this study.

CONCLUSION

Traditionally, epidemiologists and disease ecologists have focused on $R_0 > 1$ as a threshold for disease invasion (e.g. Anderson & May 1991; Diekmann & Heesterbeek 2000). We have shown that in metapopulations the relationship between invasion of disease and an individual-level R_0 is often weak. Even for very large values of R_0, a pandemic is unlikely if the expected number of times an individual will move between groups during their infectious lifetime (μ/γ) is low (Fig. 2). Pandemics in structured populations require both within-group and between-group transmission, and the group-level reproductive number R_* is a better predictor than the individual-level R_0 for these systems (Fig. 4). Results from our individually-based stochastic model support the analytical results of Ball et al. (Ball *et al.* 1997; Ball & Neal 2002; Ball *et al.* 2004), which proved that $R_* > 1$ is the threshold for disease invasion in a population with group

structure. As a general rule of thumb, the individual-level R_0 must be greater than one and the expected number of group changes while infectious (μ/γ) multiplied by the average group size must be greater than one for a pandemic to occur (Fig. 2b).

Chronic diseases with longer infectious periods allow for more mixing to occur between groups. As a result, chronic diseases will perceive more thoroughly mixed host populations and exhibit dynamics that are closer to those predicted by mean-field models than acute diseases (Fig. 1). For the same R_0, chronic diseases are more likely to invade structured populations than slow diseases. 'Slow' and 'fast' diseases are relative terms: a fast, acute disease in a host population with frequent movement between groups may well behave like a relatively slow disease in a population with less frequent movement. The probability of a pandemic in a structured population is thus an emergent property of the interaction of host and parasite demography and behavior, incorporating a dimension of host behavioral susceptibility arising from group size and movement rates. The results presented here, and in a recent paper by Lloyd-Smith et al. (2004), suggest that when contact, movement, birth and death processes occur on a timescale similar to that of the disease (i.e. the infectious period), these processes should be incorporated mechanistically into disease models.

ACKNOWLEDGEMENTS

This research was funded by the NSF-NIH Ecology of Infectious Disease Grant DEB-0090323 (PCC and WMG), NIH-NIDA Grant R01-DA10135 (JLS and WMG), and a James S. McDonnell Foundation 21st Century Science Initiative Award (WMG). Previous versions of this manuscript were greatly improved by the comments of Wendy Turner, Shirli Bar-David, George Wittemyer, Charles Nunn, Molly Smith, and three anonymous reviewers.

REFERENCES

Altizer S., Nunn C.L., Thrall P.H., Gittleman J.L., Antonovics J., Cunningham A.A., Dobson A.P., Ezenwa V., Jones K.E., Pedersen A.B., Poss M. & Pulliam J.R.C. (2003) Social organization and parasite risk in mammals: Integrating theory and empirical studies. *Annual Review of Ecology Evolution and Systematics*, 34, 517-547.

Anderson E.C. (1995) Morbillivirus infections in wildlife (in relation to their population biology and disease control in domestic animals). *Veterinary Microbiology*, 44, 319-332.

Anderson R.M. & May R.M. (1991) *Infectious Diseases of Humans: Dynamics and Control*. Oxford University Press, Oxford.

Ball F. (1999) Stochastic and deterministic models for SIS epidemics among a population partitioned into households. *Mathematical Biosciences*, 156, 41-67.

Ball F. & Lyne O.D. (2001) Stochastic multi-type SIR epidemics among a population partitioned into households. *Advances in Applied Probability*, 33, 99-123.

Ball F., Mollison D. & Scalia-Tomba G. (1997) Epidemics with two levels of mixing. *The Annals of Applied Probability*, 7, 46-89.

Ball F. & Neal P. (2002) A general model for stochastic SIR epidemics with two levels of mixing. *Mathematical Biosciences*, 180, 73-102.

Ball F.G., Britton T. & Lyne O.D. (2004) Stochastic multitype epidemics in a community of households: Estimation of threshold parameter R* and secure vaccination coverage. *Biometrika*, 91, 345-362.

Begon M., Hazel S.M., Telfer S., Bown K., Carslake D., Cavanagh R., Chantrey J., Jones T. & Bennett M. (2003) Rodents, cowpox virus and islands: densities, numbers and thresholds. *Journal of Animal Ecology*, 72, 343-355.

Bouma A., de Jong M.C.M. & Kimman T.G. (1995) Transmission of pseudorabies virus within pig-populations is independent of the size of the population. *Preventive Veterinary Medicine*, 23, 163-172.

Cain M.L., Nathan R. & Levin S.A. (2003) Long-distance dispersal. *Ecology*, 84, 1943-1944.

Cote I.M. & Poulin R. (1995) Parasitism and group-size in social animals - a metaanalysis. *Behavioral Ecology*, 6, 159-165.

Cross P.C., Lloyd-Smith J.O., Bowers J., Hay C., Hofmeyr M. & Getz W.M. (2004) Integrating association data and disease dynamics in a social ungulate: bovine tuberculosis in African buffalo in the Kruger National Park. *Annales Zoologici Fennici*, 41, 879-892.

Diekmann O. & Heesterbeek J.A.P. (2000) *Mathematical Epidemiology of Infectious Diseases: Model Building, Analysis and Interpretation*. John Wiley & Sons Ltd., Chichester, England.

Freeland W.J. (1976) Pathogens and the evolution of primate sociality. *Biotropica*, 8, 12-24.

Fulford G.R., Roberts M.G. & Heesterbeek J.A.P. (2002) The metapopulation dynamics of an infectious disease: Tuberculosis in possums. *Theoretical Population Biology*, 61, 15-29.

Getz W.M. & Pickering J. (1983) Epidemic models: thresholds and population regulation. *American Naturalist*, 121, 892-898.

Gyllenberg M. & Metz J.A.J. (2001) On fitness in structured metapopulations. *Journal of Mathematical Biology*, 43, 545-560.

Hagenaars T.J., Donnelly C.A. & Ferguson N.M. (2004) Spatial heterogeneity and the persistence of infectious diseases. *Journal of Theoretical Biology*, 229, 349-359.

Hess G. (1996) Disease in metapopulation models: Implications for conservation. *Ecology*, 77, 1617-1632.

Keeling M.J. (1999) The effects of local spatial structure on epidemiological invasions. *Proceedings of the Royal Society of London Series B-Biological Sciences*, 266, 859-867.

Keeling M.J. & Gilligan C.A. (2000) Metapopulation dynamics of bubonic plague. *Nature*, 407, 903-906.

Keeling M.J. & Grenfell B.T. (2000) Individual-based perspectives on R-0. *Journal of Theoretical Biology*, 203, 51-61.

Keeling M.J. & Rohani P. (2002) Estimating spatial coupling in epidemiological systems: a mechanistic approach. *Ecology Letters*, 5, 20-29.

Koenig W.D., VanVuren D. & Hooge P.N. (1996) Detectability, philopatry, and the distribution of dispersal distances in vertebrates. *Trends in Ecology & Evolution*, 11, 514-517.

Lloyd-Smith J.O., Getz W.M. & Westerhoff H.V. (2004) Frequency-dependent incidence in models of sexually transmitted diseases: portrayal of pair-based transmission and effects of illness on contact behaviour. *Proceeding of the Royal Society of London Series B Biological Sciences*, 271, 625-634.

McCallum H., Barlow N. & Hone J. (2001) How should pathogen transmission be modelled? *Trends in Ecology and Evolution*, 16, 295-300.

Metz J.A.J. & Gyllenberg M. (2001) How should we define fitness in structured metapopulation models? Including an application to the calculation of evolutionarily stable dispersal strategies. *Proceedings of the Royal Society of London Series B-Biological Sciences*, 268, 499-508.

Moller A.P., Dufva R. & Allander K. (1993) Parasites and the evolution of host social-behavior. In: *Advances in the Study of Behavior, Vol 22*, pp. 65-102

Nathan R., Perry G., Cronin J.T., Strand A.E. & Cain M.L. (2003) Methods for estimating long-distance dispersal. *Oikos*, 103, 261-273.

Nunn C.L. (2002) A comparative study of leukocyte counts and disease risk in primates. *Evolution*, 56, 177-190.

Nunn C.L., Altizer S., Jones K.E. & Sechrest W. (2003a) Comparative tests of parasite species richness in primates. *American Naturalist*, 162, 597-614.

Nunn C.L., Gittleman J.L. & Antonovics J. (2000) Promiscuity and the primate immune system. *Science*, 290, 1168-1170.

Nunn C.L., Gittleman J.L. & Antonovics J. (2003b) A comparative study of white blood cell counts and disease risk in carnivores. *Proceedings of the Royal Society of London Series B-Biological Sciences*, 270, 347-356.

Park A.W., Gubbins S. & Gilligan C.A. (2001) Invasion and persistence of plant parasites in a spatially structured host population. *Oikos*, 94, 162-174.

Park A.W., Gubbins S. & Gilligan C.A. (2002) Extinction times for closed epidemics: the effects of host spatial structure. *Ecology Letters*, 5, 747-755.

Plowright W. (1982) The effects of rinderpest and rinderpest control on wildlife in Africa. *Symp. Zool. Soc. Lond.*, 50, 1-28.

Sinclair A.R.E. (1977) *The African Buffalo*. University of Chicago Press, Chicago.

Stanko M., Miklisova D., de Bellocq J.G. & Morand S. (2002) Mammal density and patterns of ectoparasite species richness and abundance. *Oecologia*, 131, 289-295.

Swinton J., Harwood J., Grenfell B.T. & Gilligan C.A. (1998) Persistence thresholds for phocine distemper virus infection in harbour seal Phoca vitulina metapopulations. *Journal of Animal Ecology*, 67, 54-68.

Tella J.L. (2002) The evolutionary transition to coloniality promotes higher blood parasitism in birds. *Journal of Evolutionary Biology*, 15, 32-41.

Thrall P.H., Antonovics J. & Dobson A.P. (2000) Sexually transmitted diseases in polygynous mating systems: prevalence and impact on reproductive success. *Proceedings of the Royal Society of London Series B-Biological Sciences*, 267, 1555-1563.

Waser P.M., Creel S.R. & Lucas J.R. (1994) Death and disappearance - estimating mortality risks associated with philopatry and dispersal. *Behavioral Ecology*, 5, 135-141.

Wilson E.B. & Worcester J. (1945) The spread of an epidemic. *Proceedings of the National Academy of Sciences*, 31, 327-333.

Figure 1. Disease invasion depends upon population structure (green circles: 1 group of 1000 individuals; red points: 25 groups of 40 individuals; blue crosses: 100 groups of 10 individuals) and the duration of the infectious period. A mean-field model of one group (green circles) is a worse approximation of a structured population for an acute disease with $\gamma = 0.1$ (a) than a chronic disease with $\gamma = 0.01$ (b). For both diseases $\beta/\gamma = 5$, but the slow disease causes more infections in the structured population. Lines represent the mean of 100 simulations. Simulations with 25 or 100 groups were run on a toroidal spatial structure with a movement probability μ of 0.01, such that μ/γ=0.1 (a) or 1 (b).

Figure 2. The interaction of movement (μ), transmission (β), and group size determines the mean proportion of the population that becomes infected. In (a) β varied from 0.2 to 2 while group size was fixed at 10. In (b) group size was increased from 5 to 200 while β was fixed at 2 (β/γ=20). Increasing β/γ only affected the proportion infected when movement was frequent (a). Larger group sizes require less movement for the disease to invade (b). Each parameter set was simulated 1000 times on an 11x11 toroidal array of groups with a constant recovery probability γ of 0.1.

Figure 3. Histograms of the proportion of individuals infected during an epidemic for different transmission (β) and movement (μ) values scaled by the probability of disease recovery (γ). Each parameter set was simulated 1000 times on an 11x11 toroidal array of groups with 10 individuals each and a recovery probability γ of 0.1.

Figure 4. $\hat{R}_0$ can be substantially greater than one and yet not cause a pandemic (a), whereas $\hat{R}_*$ is a much better single predictor of the mean proportion of individuals infected (b). Each line represents a fixed transmission parameter β and a range of movement probabilities from zero to one (increasing from left to right) sampled on a log scale. Each parameter set was simulated 1000 times on an 11x11 toroidal array of groups with 10 individuals each and a recovery probability γ of 0.1.

a)

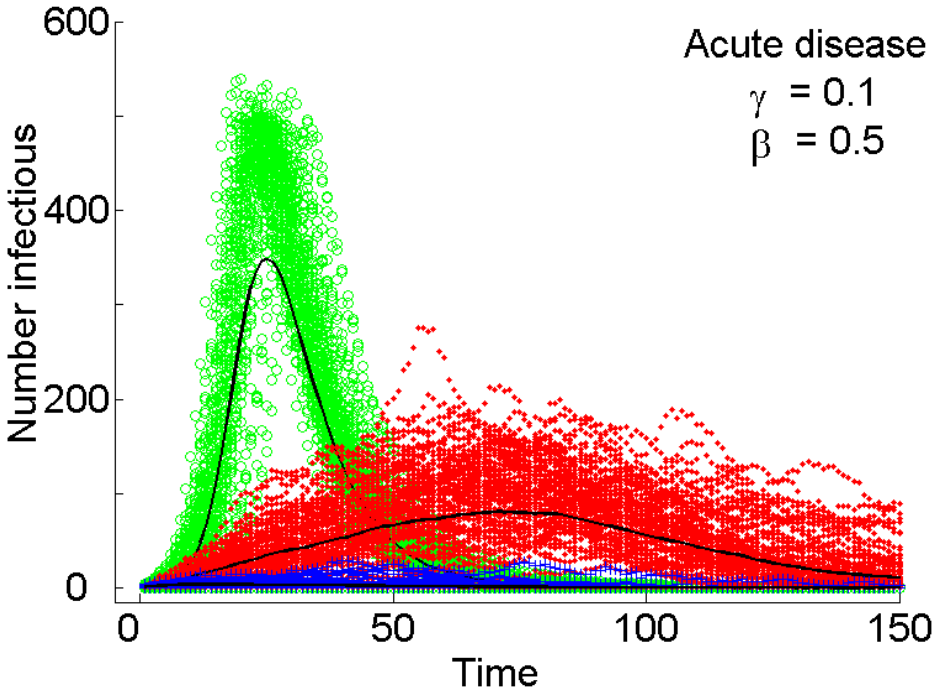
Acute disease
γ = 0.1
β = 0.5
Number infectious
Time
0
200
400
600
0
50
100
150

b)

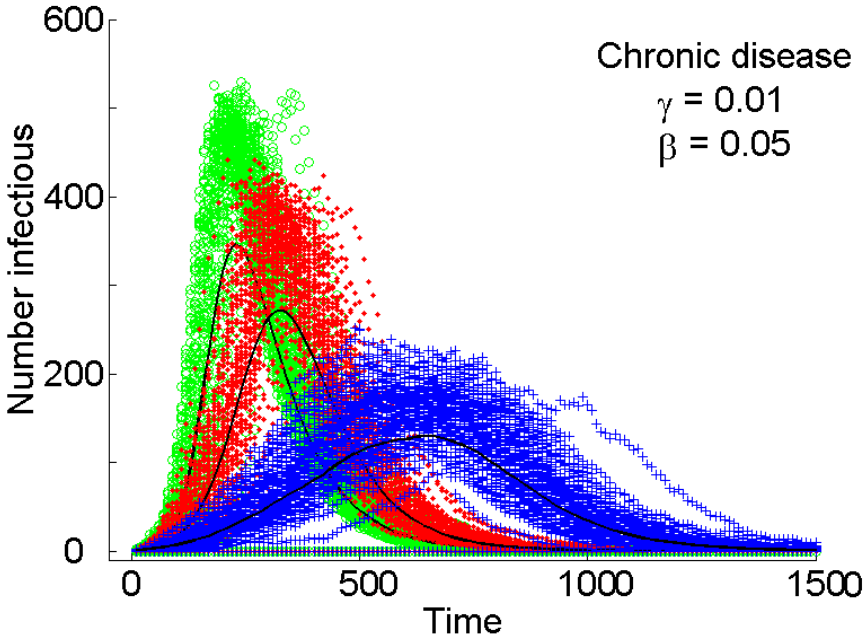
Chronic disease
γ = 0.01
β = 0.05
Number infectious
Time
0
200
400
600
0
500
1000
1500

Figure 1

a)

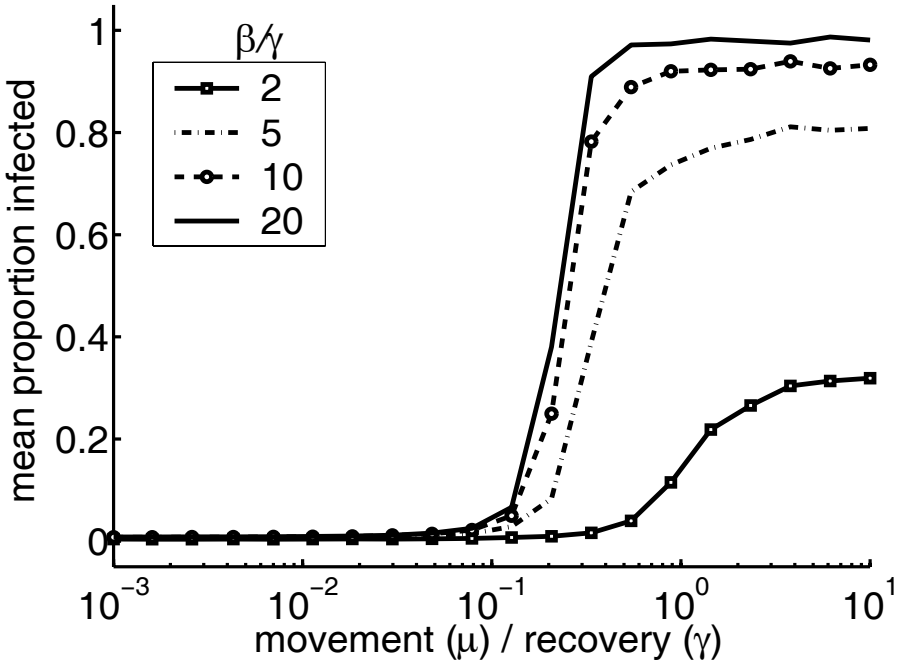
β/γ
2
5
10
20
mean proportion infected
movement (μ) / recovery (γ)

b)

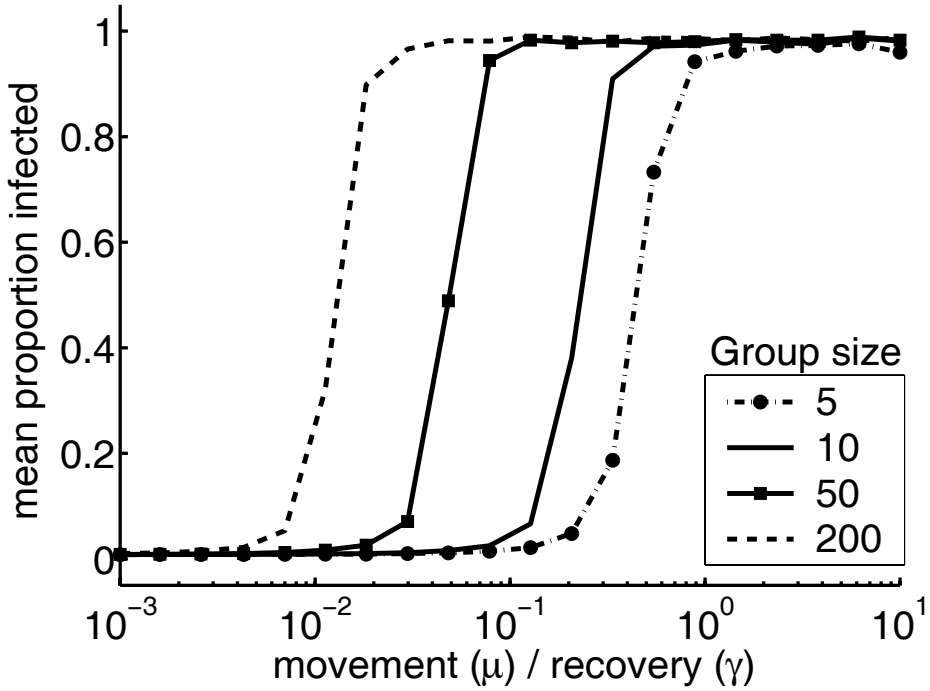
Group size
5
10
50
200
mean proportion infected
movement (μ) / recovery (γ)

Figure 2.

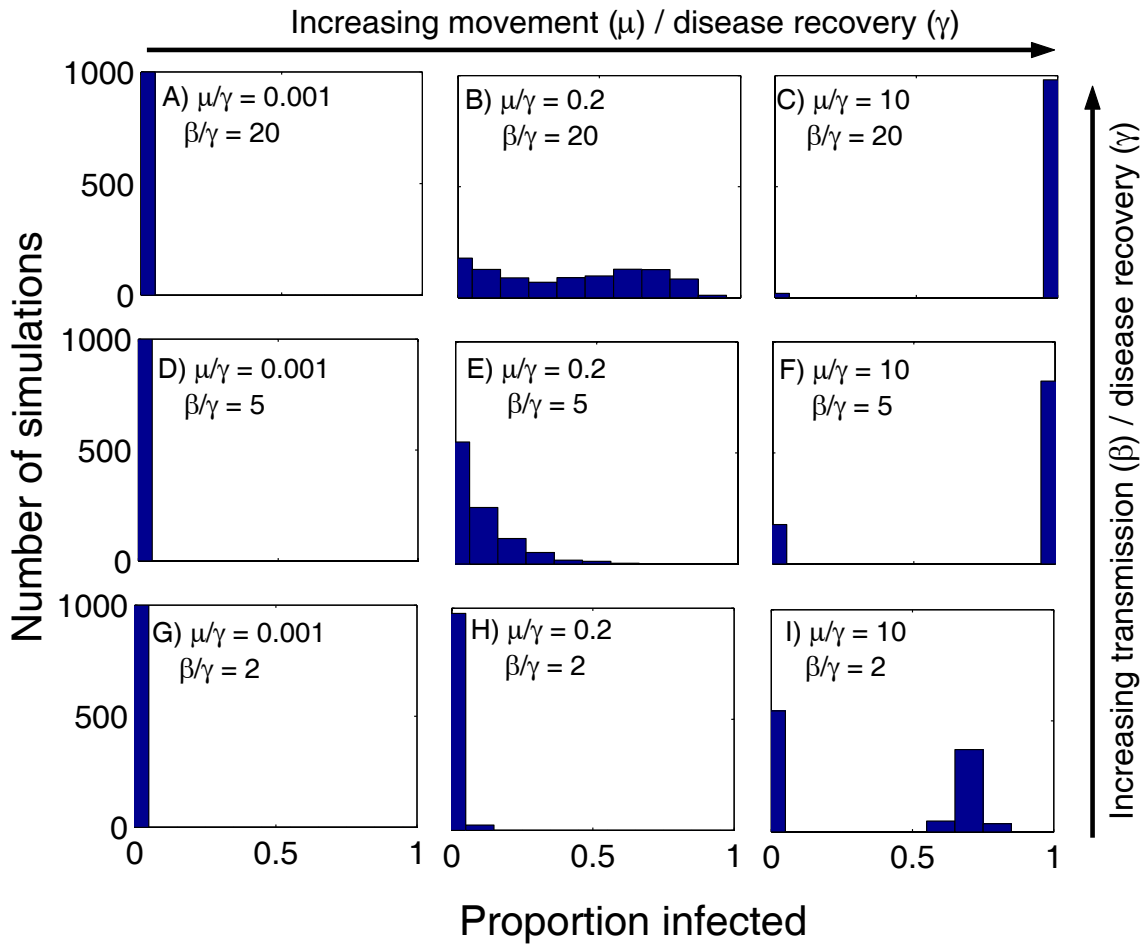
Increasing movement (μ) / disease recovery (γ)
Increasing transmission (β) / disease recovery (γ)
Number of simulations
Proportion infected
A) μ/γ = 0.001
β/γ = 20
B) μ/γ = 0.2
β/γ = 20
C) μ/γ = 10
β/γ = 20
D) μ/γ = 0.001
β/γ = 5
E) μ/γ = 0.2
β/γ = 5
F) μ/γ = 10
β/γ = 5
G) μ/γ = 0.001
β/γ = 2
H) μ/γ = 0.2
β/γ = 2
I) μ/γ = 10
β/γ = 2
1000
500
0
0
0.5
1

Figure 3

a)

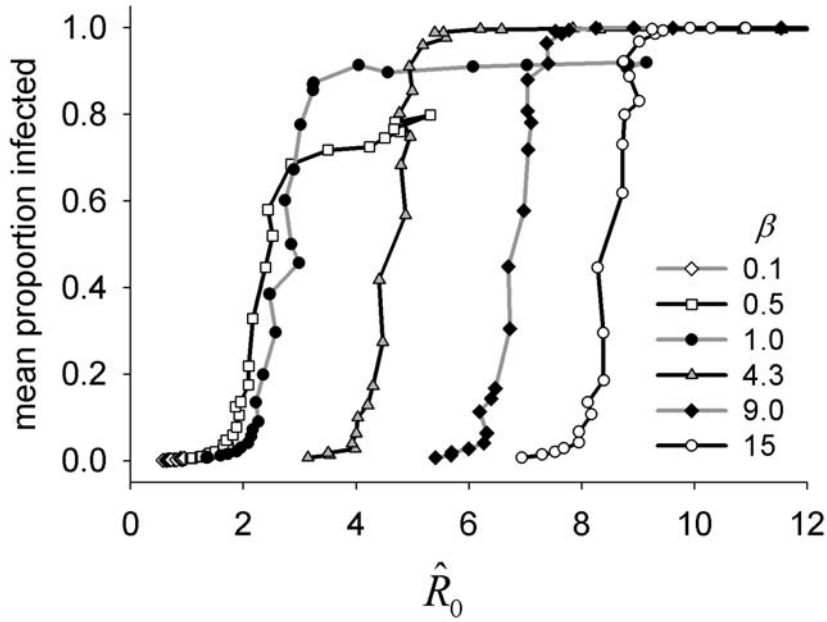
mean proportion infected
1.0
0.8
0.6
0.4
0.2
0.0
0
2
4
6
8
10
12
$\hat{R}_0$
β
0.1
0.5
1.0
4.3
9.0
15

b)

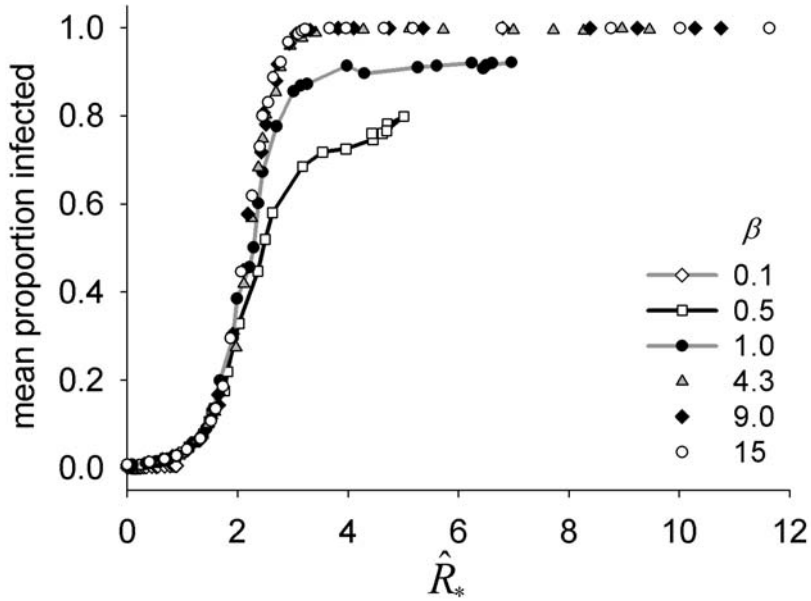
mean proportion infected
1.0
0.8
0.6
0.4
0.2
0.0
0
2
4
6
8
10
12
$\hat{R}_*$
β
0.1
0.5
1.0
4.3
9.0
15

Figure 4.

SUPPLEMENTARY MATERIAL

In the main text we focused primarily on an 11x11 toroidal array of groups with differing group sizes, and hence varying population sizes. Here we expand our analysis to investigate the effect of total population size while group size is kept constant by varying the number of groups. The effect of population size is minimal provided the group size remains fixed (Fig. S1a). At low values of μ/γ though, the proportion infected is higher for the 5x5 array than the 11x11 or 21x21 array simply because the initial herd represents a greater proportion of the population. The difference shown in Fig. 2b thus can be interpreted as a group size effect rather than an effect of increasing total population size.

We also investigated the effect of two other spatial configurations: a loop with nearest-neighbor movement and a spatially implicit array where an individual could move to any other group in one time step. As expected, disease invasion of the loop array requires a higher μ/γ ratio than invasion of the torus due to the depletion of susceptible groups (Fig. S1b). On a loop an infected individual dispersing from any given group has only two neighboring groups (compared to four in the torus) that may have been infected already by a previously dispersing individual. In contrast, invasion of the spatially implicit metapopulation requires less host movement than the torus because all groups are neighbors, thus minimizing the depletion effect by maximizing the number of neighboring groups.

Finally, we present a more complete picture of the relationships among $\hat{R}_0$, $\hat{R}_*$ and the mean proportion infected than shown in Fig. 4. Similar to Fig. 4, we simulated range of transmission and movement probabilities on an 11x11 toroidal array of groups with 10 individuals each. In contrast to Fig. 4, in Fig. S2 each line represents a fixed

movement probability, but a range of transmission coefficients. When movement is infrequent, higher transmission rates cause an increase in $\hat{R}_0$, but $\hat{R}_*$ and the mean proportion infected are relatively unaffected. Increasing the movement probability increases $\hat{R}_*$, for a given value of β. Note that when $\hat{R}_0$ is near one then both $\hat{R}_*$ and the average proportion infected are low: if the disease is likely to die out within a patch ($\hat{R}_0 \approx 1$) more frequent movement will not lead to a pandemic. When $\hat{R}_0$ is greater than one it is not a strong predictor of the mean proportion infected because the penetration of the disease into the metapopulation depends upon $\hat{R}_*$ and the probability of host movement. For a pandemic to occur both $\hat{R}_0$ and $\hat{R}_*$ must be significantly greater than one (Fig. S2).

Note that there are regions of the $\hat{R}_0$ - $\hat{R}_*$ parameter space where lines are absent. If $\hat{R}_0 \leq 1$ then $\hat{R}_*$ is not greater than one 1 because the disease is unlikely to invade multiple groups if extinction is likely within the initial group. Further, for the simulations we conducted with a recovery rate of 0.1, $\hat{R}_0$ was usually less than the group size because of the competition amongst infectious individuals to infect the remaining susceptibles within the group. $\hat{R}_0$ can exceed the group size, however, if movement rates are high and recovery rates are low.

Fig. S1. The mean proportion of the population that becomes infected hardly depends on the number of groups, or individuals, in the population (a), but does depend on the spatial array (b). In (a) the spatial configuration is a torus, but the number of groups (and hence total population size) varies. In (b) all simulations have 121 groups in different spatial configurations. Each parameter set was simulated 1000 times, with a group size of ten and a recovery probability γ of 0.1.

Figure S2. The mean proportion of individuals that are infected is a function of the average $\hat{R}_*$ and average $\hat{R}_0$. Each line represents averages of 1000 simulations with a fixed movement probability and varying transmission rates. Note $\hat{R}_0$ can be substantially greater than one and yet not cause a pandemic if movement is infrequent. All parameter sets were simulated on an 11x11 toroidal array of groups with 10 individuals each and a recovery probability γ of 0.1.

a)

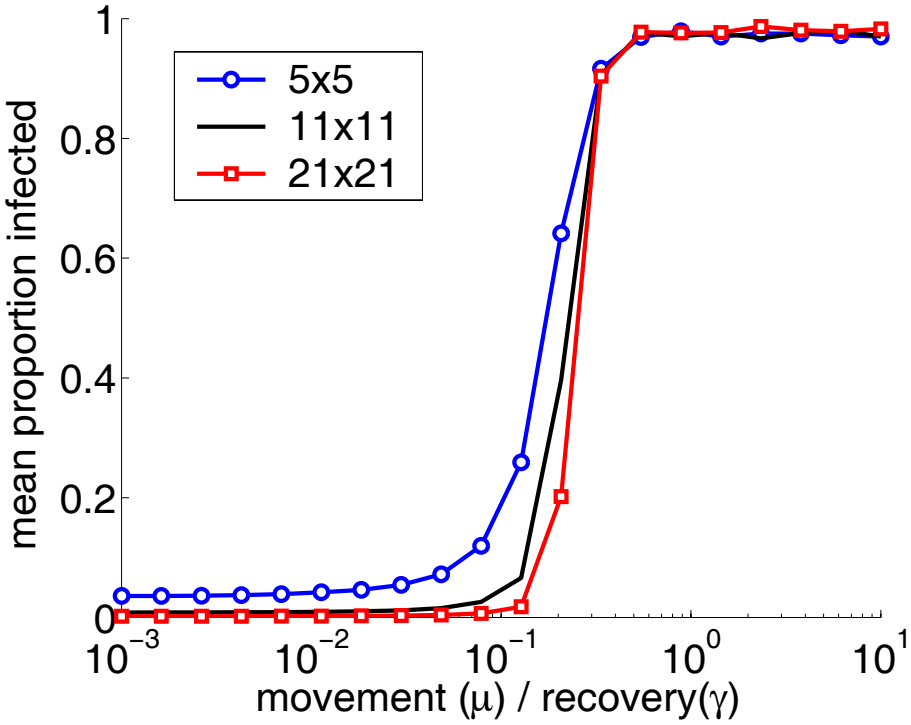
5x5
11x11
21x21
mean proportion infected
movement (μ) / recovery(γ)

b)

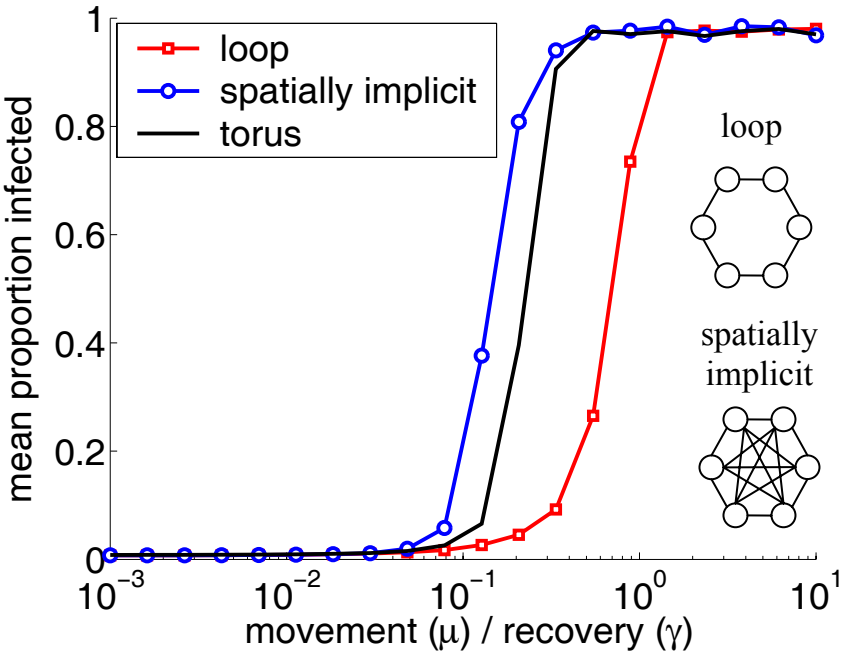
loop
spatially implicit
torus
loop
spatially implicit
mean proportion infected
movement (μ) / recovery (γ)

Figure S1.

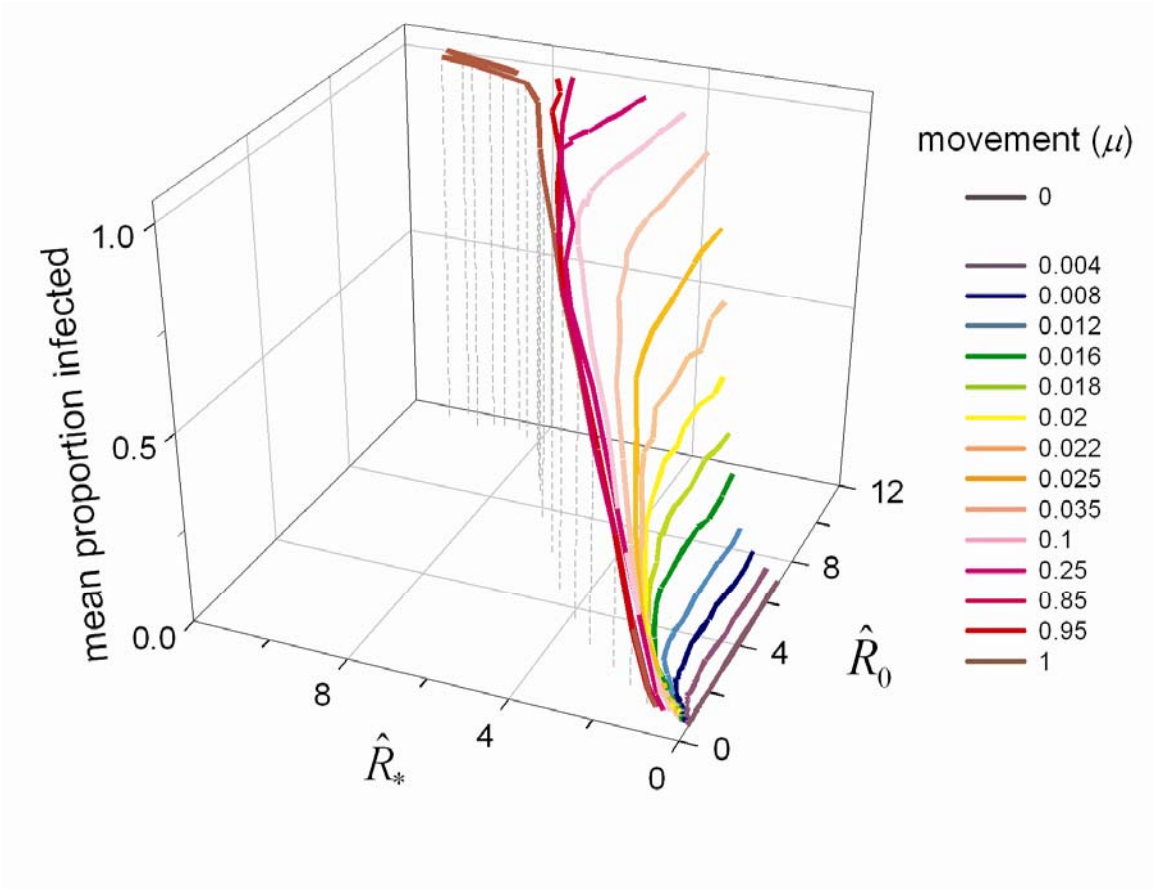
mean proportion infected
1.0
0.5
0.0
8
4
0
$\hat{R}_*$
0
4
8
12
$\hat{R}_0$
movement (μ)
0
0.004
0.008
0.012
0.016
0.018
0.02
0.022
0.025
0.035
0.1
0.25
0.85
0.95
1

Figure S2.